A CCBA DESCRIPTION OF THE (p, t) REACTION TO LOW-LYING 0^+ STATES IN THE Ge ISOTOPES

A. BECKER, C. ALDERLIESTEN, E.A. BAKKUM, K. VAN DER BORG,
C.P.M. VAN ENGELEN, L. ZYBERT* and R. KAMERMANS

Fysisch Laboratorium, Rijksuniversiteit Utrecht, P.O. Box 80.000, 3508 TA Utrecht, The Netherlands

Abstract: Differential cross sections for the (p, t) reaction to 0^+ states in the even Ge isotopes have been measured at an incident energy ($E_p = 13$ MeV) where the triton energy is below the Coulomb barrier. The data are described by a coupled-channels calculation with wave functions consisting of neutron configurations only. Sequential transfer processes can explain the anomalies, which have led previously to the introduction of shape isomerism or proton excitations.

1. Introduction

The large amount of data obtained in the past years about the Ge isotopes and neighbouring nuclei has revealed several interesting phenomena, especially for the even–even nuclei. The level schemes at low excitation are strongly reminiscent of that of an anharmonic vibrator. Also the electromagnetic properties of those levels indicate appreciable collectivity. The behaviour of the first excited 0^+ state (0_2^+), however, does not fit in a vibrational picture. The energy of this state shows considerable deviations from the expectation for a vibrator and has a striking minimum at neutron number $N = 40$ (in ^{72}Ge it is even below the 2_1^+ state). In the Se isotopes rotational bands have been found, which are possibly built on the 0_2^+ state, indicating a (prolate or triaxial) deformation of these states. All this information points to the direction of an interplay between different modes of collective excitation. A review of the most salient features can be found in ref. [1]).

On the other hand, (p, d) [2]) and (d, p) [3]) experiments on the Ge isotopes and neighbouring nuclei have revealed that for neutron numbers $N = 38$–50 mainly the $2p_{1/2}$ and $1g_{9/2}$ orbits are active for the neutrons, although the $2p_{3/2}$ and $1f_{5/2}$ orbits are not completely filled. For the protons the $2p_{3/2}$ and $1f_{5/2}$ orbits are the main active ones [4]). These facts suggest that the lowest excited states might be described with relatively simple shell-model wave functions.

---

* Permanent address: Institute of Nuclear Physics, Cracow, Poland.

Evidence for both collective and single-particle aspects has been deduced from the peculiar behaviour of the low-lying excited 0^+ states in the even Ge isotopes observed in (p, t)[5-7] and (t, p)[8-10] reactions and recently also in (d, ^{6}Li)[11] and (^{6}Li, d)[12]. It was found that e.g. the 0_2^+ state in ^{72}Ge is relatively strongly excited in the (p, t) reaction, whereas the (t, p) transition to the same state is much weaker and has an anomalously shaped angular distribution. For the ^{74}Ge(0_2^+) state the situation is reversed. Here the (t, p) transition has a large strength and a normal angular distribution, whereas the (p, t) reaction is weak and anomalous. Such features have also been observed for other 0^+ states although less pronounced. In analogy with similar variations in the (p, t) and (t, p) strength observed in the Sm isotopes [13,14] these phenomena have been related to a coexistence of spherical and deformed shapes in a single nucleus and a transition from spherical to deformed shapes with increasing neutron number [1,8,9,15].

Alternative microscopic explanations have been proposed based on the orthogonality of the 0^+ ground and first-excited states in either the neutron[5] or the proton[1,12] configurations. In both cases simple two-component wave functions have been used with amplitudes extracted from experimental data. These models can explain the relative strengths observed in the two-neutron (and α-particle) transfer reactions, but the anomalous shapes of some of the angular distributions have not been reproduced so far. Also the absolute cross sections are not reproduced by DWBA calculations with these wave functions. The experimental cross sections are enhanced with respect to the calculations by a factor of about 10 [ref.[5]].

In the present work the (p, t) reaction on the Ge isotopes has been studied at a much lower proton energy ($E_p = 13$ MeV) than used previously, which leads to triton energies well below the Coulomb barrier. It has been shown by Iwasaki[16] that at sub-Coulomb energies the shape of the angular distribution becomes more sensitive to the microscopic structure of the transferred neutron pair. The tritons, due to their long wavelength, probe a larger part of the outer tail of the form factor, which is most sensitive to the orbital angular momentum of the single-particle orbits involved. Therefore one can expect to obtain more information about the microscopic structure of the nuclear states excited in such a reaction.

In our analysis of the $L = 0$ angular distributions, it was found necessary to include two-step processes in the calculations. In this approach it was possible to obtain a good description of both the shape and the absolute magnitude of the angular distributions using simple shell-model wave functions.

Part of the results has been published in a preliminary report[17].

2. Experimental procedure

The (p, t) reaction on the ^{72,74,76}Ge isotopes was investigated with a 13 MeV proton beam from the 7 MV EN-tandem accelerator in Utrecht with currents of about 500 nA. Targets of isotopically enriched ^{72,74,76}Ge (98%, 99% and 74%,

respectively) with thicknesses of about 250 μg/cm^2 were either self-supporting or evaporated onto 30 μg/cm^2 thick carbon backings. The tritons were momentum analyzed in an Enge split-pole spectrograph and detected in a gas-ionization chamber of the type developed in Rochester [18]). The detector consists of two proportional counters with resistive wires for position read-out. A 10 cm wide ionization section between the two wires is used to provide an energy loss signal, while the remaining 15 cm of the 25 cm deep chamber determines the residual energy of the particles. The 25 cm long detector was positioned with the wires at an angle of 42° with respect to the focal plane of the spectrograph, such that the average trajectory of the incoming particles is perpendicular to the position sensitive wires. In this position the detector effectively covers a range of 30 cm in the focal plane. The detector was filled with isobutane at a pressure of 125 Torr, which was not enough to stop all tritons completely, but sufficient to provide an adequate separation of tritons from protons, deuterons and α-particles. Although this detector was originally designed for heavy ions it proved to be useful also for the present purposes. The 1.2 mm intrinsic position resolution corresponds to 6 keV for 4 MeV tritons, which is negligible compared to the 30–50 keV total energy resolution determined by the energy loss in the target. The detector could also handle the high count rates (up to $\approx 2 \times 10^4$ s^{-1}) of elastically scattered protons at forward angles which is probably a virtue of the small amount of ionization of these particles.

All primary signals from the detector were stored event by event on magnetic tape by a PDP 11/34 computer. The particle selection and the construction of momentum spectra for the tritons were performed off-line by means of a PDP 11/70 computer.

Angular distributions were measured in 10° steps from $\theta_{lab} = 20°$ to 140°. The solid angle of the spectrograph was 2.4 msr while the opening angle in the reaction plane was 2.8°. For the reaction on ^{76}Ge two settings of the spectrograph magnetic field had to be used in order to cover an excitation energy range of 1.5 MeV. The relative normalization of the different runs was obtained by monitoring the elastically scattered protons with a solid state detector at a fixed angle of $\theta_{lab} = 120°$. Absolute cross sections with an estimated accuracy of 15% were obtained by comparing elastic scattering cross sections for 13 MeV protons, measured in an angular range from $\theta_{lab} = 15°$ to 30°, with existing data at 14.5 MeV [ref. [19])] and 11 MeV [ref. [20])] and with optical model calculations.

3. Experimental results

Triton spectra for the three reactions, obtained at an angle of $\theta_{lab} = 90°$, are shown in fig. 1. Final states up to an excitation energy of 1.5 MeV in ^{74}Ge and 1 MeV in ^{72}Ge were observed while in ^{70}Ge only the ground state could be measured. Higher excited states were not observable because the corresponding triton energies are too low in comparison with the Coulomb barrier. Five $0^+ \rightarrow 0^+$
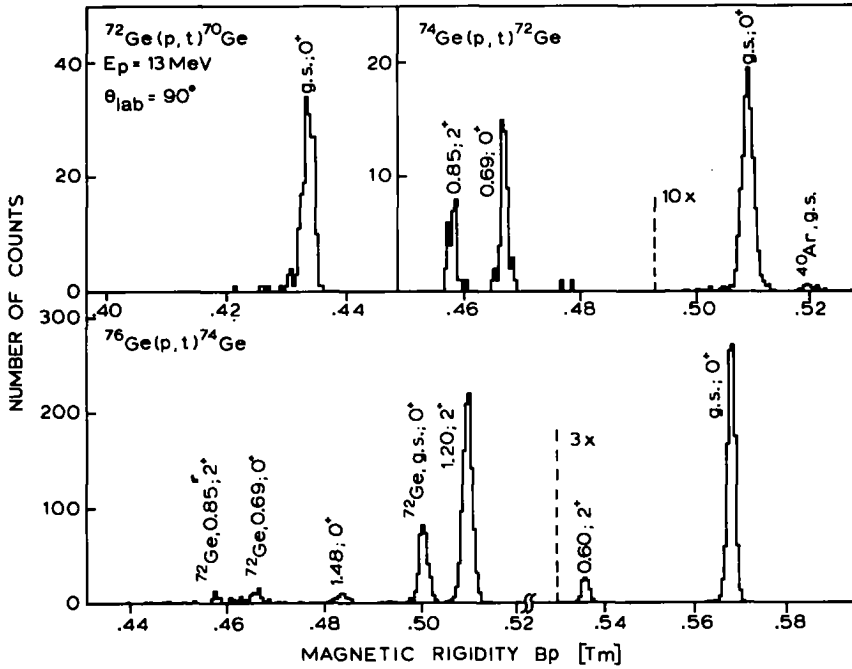
Fig. 1. Spectra of the ^{72,74,76}Ge(p, t)^{70,72,74}Ge reactions, measured at $E_p = 13$ MeV and $\theta_{lab} = 90°$.

transitions were investigated among which the "normal" transition to the 0_2^+ state in ^{72}Ge and the "anomalous" transition to ^{74}Ge(0_2^+). Also three $0^+ \rightarrow 2^+$ transitions were observed. The 4_1^+ state in ^{74}Ge at an excitation energy of $E_x = 1.464$ MeV was not resolved from the 0_2^+ state at 1.483 MeV, but it is expected to be only weakly excited. A maximum cross section of 0.15 μb/sr for the 4_1^+ state was obtained by scaling the calculated angular distribution (DWBA with a $1g_{9/2}^2$ form factor) with the ratio of experimental and calculated cross sections at 26 MeV [ref. [6])], where the 4_1^+ and 0_2^+ could be separated. This value is small compared to the observed $d\sigma/d\Omega$(max) = 2.8 μb/sr for the 0_2^+ state.

The sub-Coulomb angular distributions show a clear diffraction-like pattern (see fig. 2). The contribution from compound nucleus decay is expected to be small. The total cross section for all triton exit channels in the reaction 13 MeV p + ^{74}Ge, calculated with the statistical model code STATIS [21]), is only 2 μb while the main part of the total flux (98% of the reaction cross section) is going into the neutron exit channels.

The general behaviour of the $L = 0$ transitions (see fig. 2) is similar to what has been observed at higher proton energies. The ratio of the cross sections for the 0_2^+ and ground-state transitions is indeed much larger for ^{72}Ge than for ^{74}Ge (see also table 1) but it is in both cases reduced with respect to the ratio at higher proton
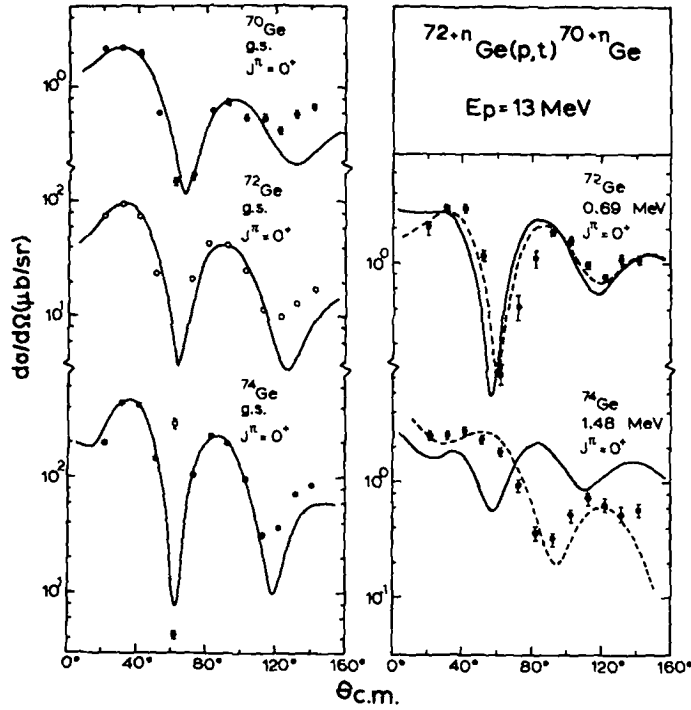
Fig. 2. Angular distributions for the ^{72,74,76}Ge(p, t)^{70,72,74}Ge reactions. The curves are results from CCBA calculations with the wave functions of table 3, scaled with the enhancement factors given in table 1. The dashed curves for the 0_2^+ states were calculated with the modified ^{74}Ge wave functions.

energies due to the influence of the Coulomb barrier. The shape of the angular distributions is very similar for all g.s. → g.s. transitions, while that of the angular distribution for ^{74}Ge(0_2^+) strongly deviates. But also the transition to ^{72}Ge(0_2^+) is different from the g.s. → g.s. transitions, which can be seen most clearly in fig. 3 explained in the next section.

4. Single-step DWBA analysis

In first instance single-step DWBA calculations were performed for the $L = 0$ (p, t) angular distributions using the zero-range computer code DWUCK-IV [22]). Parameters used for the optical model potentials are listed in table 2. These are standard sets, taken from the compilation by Perey and Perey [23]) with one exception. The depth of the real potential for the protons was changed from $V_0 = -52.8$ MeV to -57 MeV in order to effect an angular shift of about 8°, needed to reproduce the shape of the ground-state angular distributions. The effect of this modification on the absolute cross sections was less than 10%. The transferred neutrons were bound in a Woods–Saxon potential well ($r_0 = 1.28$ fm, $a_0 = 0.66$ fm) with binding

TABLE 1

Comparison of measured and calculated cross sections for 0^+ states excited in the (p, t) reaction on Ge isotopes at $E_p = 13$ MeV

Final state	$\dfrac{d\sigma}{d\Omega_{exp}}$ [a]) (μb/sr)	ε_{direct} [b])	ε_{CCBA} [c])	ε_{MAXT} [d])	ε_{SSR4} [e])
^{70}Ge (g.s.)	2.2	4.7	0.9	0.6	0.9
^{72}Ge (g.s.)	94	8.2	1.1 (1.5)	0.9	1.9
^{72}Ge (0_2^+)	3.1	4.1	2.0 (3.6)	2.2	0.7
^{74}Ge (g.s.)	425	4.8	1.8 (1.6)	1.5	2.6
^{74}Ge (0_2^+)	2.8	$\approx$30	$\approx$1.2 (1.9)	$\approx$1	$\approx$1

[a]) Differential cross section at the first maximum ($\theta_{lab} = 30°$).

[b]) Enhancement factors (ratio of experimental to calculated cross section) for the single-step DWBA calculations. The wave functions used to calculate the form factors are given in table 3 (modified set).

[c]) Enhancement factors obtained from the coupled-channels analysis with wave functions from the simple model. The values between brackets were calculated with the modified set of wave functions (see table 3).

[d]) Enhancement factors for coupled-channels calculations with shell-model wave functions from the MAXT calculations [see sect. 5 and ref. [27])].

[e]) Same as [d]) but for the SSR4 model.

energies determined according to the two-neutron separation energy prescription. The two-neutron transfer form factors, which consist of a coherent sum of $2p_{1/2}^2$ and $1g_{9/2}^2$ contributions, were calculated with the microscopic method of Bayman and Kallio [24]), where the two neutrons are assumed to be in a relative S-state. The spectroscopic amplitudes were determined from simple shell-model wave functions, to be discussed in sect. 5.

Results of these calculations are shown in fig. 3. This figure clearly illustrates the different behaviour of the angular distributions with pure $2p_{1/2}^2$ (dashed curves)

TABLE 2

Optical model parameters [a]) used in the DWBA and CCBA analyses of the (p, t) reaction on Ge isotopes at $E_p = 13$ MeV

	V	r_0	a_0	W	W_D	r_W	a_W	$V_{s.o.}$	$r_{s.o.}$	$a_{s.o.}$	r_C	Ref.
p+Ge	52.8 [b])	1.25	0.65		13.5	1.25	0.47	7.5	1.25	0.47	1.25	[31])
t+Ge	163.5	1.20	0.72	32.3		1.40	0.84	2.5	1.20	0.72	1.3	[32])
d+Ge	108	1.05	0.86		12.5	1.43	0.73	7.0	0.75	0.50	1.3	[33])
n+Ge	[c])	1.285	0.66					25 [d])				

[a]) The definition of the parameters is that of ref. [23]). V and W are in MeV, r and a in fm.

[b]) In the single-step DWBA analysis this parameter was modified to 57 MeV.

[c]) Adjusted to reproduce the binding energy of the neutron.
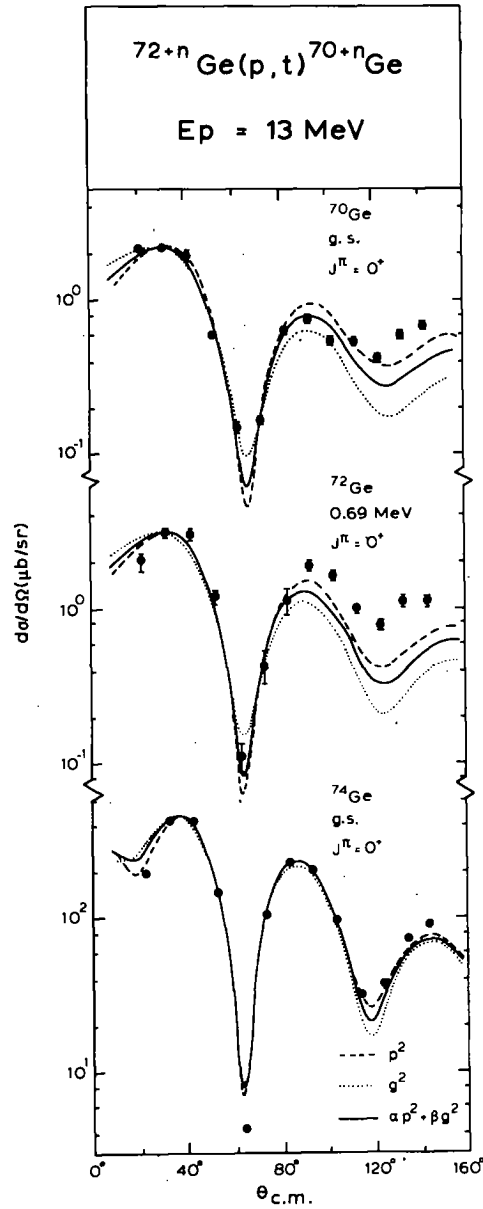
[d]) Thomas spin–orbit factor.

Fig. 3. Comparison of experimental angular distributions with single-step DWBA calculations. The dashed curves are calculated with a pure $2p_{1/2}^2$ form factor and the dotted curves with a pure $1g_{9/2}^2$ form factor, while for the solid curves a combination of $2p_{1/2}^2$ and $1g_{9/2}^2$ form factors was used, based on the wave functions of table 3. Scaling factors (ε) for the latter are given in table 1.

and pure $1g^2_{9/2}$ form factors (dotted curves) as a function of the energy of the tritons in the exit channel, which is especially manifested in the ratio of the differential cross sections at the second and the first maximum. This difference is quite large for the transition to the ^{70}Ge ground state where the triton energy is about 3 MeV, far below the Coulomb barrier of 6.5 MeV. For the transition to the ground state of ^{74}Ge at a triton energy of 5 MeV the difference is already much less significant.

A combination of $2p^2_{1/2}$ and $1g^2_{9/2}$ form factors, whose orbits are expected to dominate the two-neutron transfer on the basis of measured occupation probabilities [2,3]), gives a good description of the shape of all measured ground-state angular distributions up to the second maximum. The shape of the angular distribution of the transition to the second 0^+ in ^{72}Ge could not be reproduced with this approach. As can be seen from fig. 3, the measured angular distribution is considerably higher at the second maximum than both the $2p^2_{1/2}$ and the $1g^2_{9/2}$ curves. A destructive interference between the two components of the form factor would be needed to reproduce the experimental shape of the ^{72}Ge(0^+_2) transition which, however, would simultaneously reduce the calculated absolute cross sections considerably. The shape of the anomalous angular distribution for the ^{74}Ge(0^+_2) state cannot be described with the single-step approach.

The agreement between experimental and calculated (DWUCK) absolute cross sections can be expressed in terms of the enhancement factors ε, defined by the relation

$$\frac{d\sigma}{d\Omega_{exp}}(\theta) = \varepsilon N \frac{d\sigma}{d\Omega_{DWUCK}}(\theta), \qquad (1)$$

for the present cases ($J^\pi = 0^+ \to 0^+$; minimum isospin of initial and final states), where $N = 243$ is the zero-range normalization factor for the (p, t) reaction. Values of ε for the five $L = 0$ angular distributions are given in table 1. They were calculated with the simple shell-model wave functions to be discussed in sect. 5. Important for the present discussion is that they are around $\varepsilon = 5$ which indicates a considerable discrepancy between experimental and calculated cross sections. This fact, combined with the poor description of the shape of both 0^+_2 angular distributions motivated us to investigate the influence of two-step processes.

5. Coupled-channels analysis

5.1. CALCULATIONS WITH SIMPLE SHELL-MODEL WAVE FUNCTIONS

The most straightforward way to describe the ground states of the $^{70-76}$Ge isotopes from a shell-model point of view is to consider ^{70}Ge as an inert core, where the protons fill the $2p_{3/2}$ orbit and the neutrons the $2p_{3/2}$ and $1f_{5/2}$ orbits. The $2p_{1/2}$ and $1g_{9/2}$ orbits are starting to be filled by the neutrons in going from ^{70}Ge to ^{76}Ge. These global characteristics are in agreement with occupation probabilities of the neutron orbits extracted from (p, d) [2]) and (d, p) [3]) work. The wave functions

of the 0^+ ground states of the even isotopes and of the first $\frac{1}{2}^-$ and $\frac{9}{2}^+$ states in the odd isotopes can then be written in the following way ($n = 2, 4, 6$):

$$|^{70+n}\mathrm{Ge}(0_1^+)\rangle = \alpha_n |(2p_{1/2})_0^2 (1g_{9/2})_0^{n-2}\rangle + \beta_n |(1g_{9/2})_0^n\rangle,$$

$$|^{69+n}\mathrm{Ge}(\tfrac{1}{2}_1^-)\rangle = |2p_{1/2}(1g_{9/2})_0^{n-2}\rangle, \qquad (2)$$

$$|^{69+n}\mathrm{Ge}(\tfrac{9}{2}_1^+)\rangle = \gamma_n |(2p_{1/2})_0^2 (1g_{9/2})_{9/2}^{n-3}\rangle + \delta_n |(1g_{9/2})_{9/2}^{n-1}\rangle.$$

Only configurations with the lowest seniority have been retained. If one assumes that the proton structure is not yet excited at these low excitation energies, the wave functions of the 0_2^+ states are found from the corresponding ground-state wave functions by orthonormality:

$$|^{70+n}\mathrm{Ge}(0_2^+)\rangle = \beta_n |(2p_{1/2})_0^2 (1g_{9/2})_0^{n-2}\rangle - \alpha_n |(1g_{9/2})_0^n\rangle. \qquad (3)$$

The coefficients α_n, β_n, γ_n and δ_n were determined by solving the eigen-equation of the shell-model hamiltonian with a surface-delta two-body interaction (SDI). The strength parameter for this interaction, $A = 0.23$ MeV, and the single-particle energies, $\varepsilon(2p_{1/2}) = -10.60$ MeV, $\varepsilon(1g_{9/2}) = -10.14$ MeV, were taken from the work of De Vries [27]. The resulting wave functions are listed in table 3. Spectroscopic

TABLE 3

Wave functions used in coupled-channels calculations for the (p, t) reaction on even Ge isotopes

Nucleus	E_x (keV)	J^π	Wave function [a]
^{70}Ge	0	0^+	$|0\rangle$
^{71}Ge	0	$\frac{1}{2}^-$	$|p\rangle$
^{71}Ge	198	$\frac{9}{2}^+$	$|g\rangle$
^{72}Ge	0	0^+	$0.71|p^2\rangle - 0.71|g^2\rangle$
^{72}Ge	692	0^+	$0.71|p^2\rangle + 0.71|g^2\rangle$
^{73}Ge	0	$\frac{9}{2}^+$	$0.79|p^2g\rangle - 0.62|g^3\rangle$
^{73}Ge	67	$\frac{1}{2}^-$	$|pg^2\rangle$
^{74}Ge	0	0^+	$0.82|p^2g^2\rangle - 0.58|g^4\rangle$
^{74}Ge [b]	0	0^+	$0.50|p^2g^2\rangle - 0.87|g^4\rangle$
^{74}Ge	1483	0^+	$0.58|p^2g^2\rangle + 0.82|g^4\rangle$
^{74}Ge [b]	1483	0^+	$0.87|p^2g^2\rangle + 0.50|g^4\rangle$
^{75}Ge	0	$\frac{1}{2}^-$	$|pg^4\rangle$
^{75}Ge	200	$\frac{9}{2}^+$	$0.87|p^2g^3\rangle - 0.49|g^5\rangle$
^{76}Ge	0	0^+	$0.88|p^2g^4\rangle - 0.47|g^6\rangle$

[a] All configurations have the lowest seniority. The notation $|p^i g^j\rangle$ stands for a configuration with i neutrons in the $2p_{1/2}$ orbit and j neutrons in the $1g_{9/2}$ orbit.

[b] Modified wave functions which give a good description of the angular distribution for the $^{74}\mathrm{Ge}(0_2^+)$ state.

amplitudes were calculated from these wave functions by applying the formalism given in ref. [28]).

The contribution of two-step processes to the $L = 0$ (p, t) angular distributions has been calculated with the coupled-channels Born approximation (CCBA) code CHUCK [22]). The coupling schemes (see fig. 4) included (i) the direct (p, t) step with a form factor consisting of a coherent sum of $2p_{1/2}^2$ and $1g_{9/2}^2$ contributions, (ii) the sequential (p, d)(d, t) process via the lowest $\frac{1}{2}^-$ state in the intermediate odd Ge isotope with $2p_{1/2}$ form factors, and (iii) the (p, d)(d, t) route via the lowest $\frac{9}{2}^+$ state in the intermediate isotope with $1g_{9/2}$ form factors. The lowest $\frac{1}{2}^-$ and $\frac{9}{2}^+$ states are expected to play a dominant role in the sequential transfer, because they are strongly excited in the (p, d) reaction on the even Ge isotopes [2]). In fact, most of the $l = 1$ ($2p_{1/2}$) and $l = 4$ strength observed in the (p, d) reaction is contained in the transitions to these states.
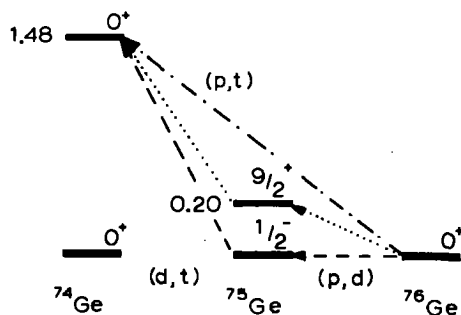

Fig. 4. Example of the coupling schemes used in the CCBA calculations. The dashed and dotted lines indicate one-neutron pickup transitions with $2p_{1/2}$ and $1g_{9/2}$ form factors, respectively, while the dash-dotted line corresponds to two-neutron pickup with a combined $2p_{1/2}^2$ and $1g_{9/2}^2$ form factor.

The correct phase factors of the spectroscopic amplitudes can be obtained from the shell-model calculations, if one takes into account the differences in the conventions used by the CCBA program and the shell-model calculations, which may occur at the following points. (i) The coupling order of orbital and intrinsic angular momenta of the single-particle orbits involved in the transfer ($1 + s = j$ or $s + 1 = j$). (ii) The sign of the radial part of the single-particle wave functions. The harmonic oscillator wave functions of the shell model usually differ by a factor $(-1)^n$, where n is the number of radial nodes, from the Woods–Saxon wave functions used in the CHUCK program. (iii) The spherical harmonics used in the angular part of the single-particle wave functions may differ by a factor $(i)^l$ [Biedenharn and Rose [25]) or Condon and Shortley [26]) convention]. Furthermore the shell-model calculations should be performed in an internally consistent way, because also there different phase conventions are in use, e.g. for the coefficients of fractional parentage.

The program CHUCK completely accounts for the angular momentum coupling. It requires, apart from the heavy-particle spectroscopic amplitudes, only coupling

strengths $S^{1/2}D_0$ (the product of light-particle spectroscopic amplitude and zero-range normalization constant) as input to calculate the absolute cross sections. Parameters for the optical model potentials used for the proton, deuteron and triton channels are listed in table 2. They were taken from the compilation of Perey and Perey [23]). No modification of these standard sets was needed. The observed angular shift between the experimental ground-state angular distributions and those calculated with the single-step DWBA appeared to be removed by the inclusion of two-step processes. The values of $S^{1/2}D_0$ were taken to be 122.5, 225 and 1560 MeV·fm$^{3/2}$ for the (p, d), (d, t) and (p, t) transitions, respectively. These values include the light-particle isospin coupling coefficients. The heavy-particle isospin coupling coefficients are 1 for the cases discussed in this paper.

The results of CCBA calculations for all measured $0^+ \rightarrow 0^+$ transitions, for the wave functions of table 3, are presented in fig. 2 (solid curves). The shapes of the angular distributions for the ground-state transitions are well-described by these calculations and the calculated absolute cross sections for all transitions are much closer to the experimental values than those calculated with the direct (p, t) process only. The enhancement factors have become much smaller; they range from 1 to 2 (see table 1). The shape of the angular distribution for the ^{72}Ge(0_2^+) state shows an angular shift of about 6° with respect to experiment. Also the ratio of the cross section at the second and the first maximum is calculated too large. With the single-step DWBA this ratio was calculated too low (see fig. 3). Apparently the relative strength of the (p, d)(d, t) route via the $\frac{1}{2}_1^-$ state, which is mainly responsible for the observed discrepancies, is overestimated in the present calculation. For ^{74}Ge(0_2^+) the strong destructive interference between the sequential $2p_{1/2}$ and $1g_{9/2}$ paths causes the calculated shape to be very sensitive to details of the wave functions. The result, shown in fig. 2, is already anomalous in shape but it does not describe the data.

A good description of the ^{74}Ge(0_2^+) angular distribution (dashed curve in fig. 2) can be obtained, however, by changing the amplitude of one component in the wave functions for ^{74}Ge as indicated in table 3. This modification simultaneously gives a considerable improvement of the shape for the ^{72}Ge(0_2^+) transition, whereas the corresponding enhancement factor becomes somewhat larger.

Fig. 5 illustrates the individual contributions of the one- and two-step processes to the total cross section for some of the transitions. From this figure it is clear that the two-step processes have a drastic effect on the net result. Especially the angular distribution for the ^{74}Ge(0_2^+) state is determined almost completely by the (destructive) interference between the two (p, d)(d, t) routes. But even for the ground-state transitions they are comparable in strength with the direct process.

Within the simple model one can also expect sequential transfer via a second $\frac{9}{2}^+$ state in the intermediate isotopes. These $\frac{9}{2}_2^+$ states have a small overlap with the ground states of both neighbouring isotopes but a considerable overlap with the 0_2^+ states. However, these states are not well known experimentally and they may well
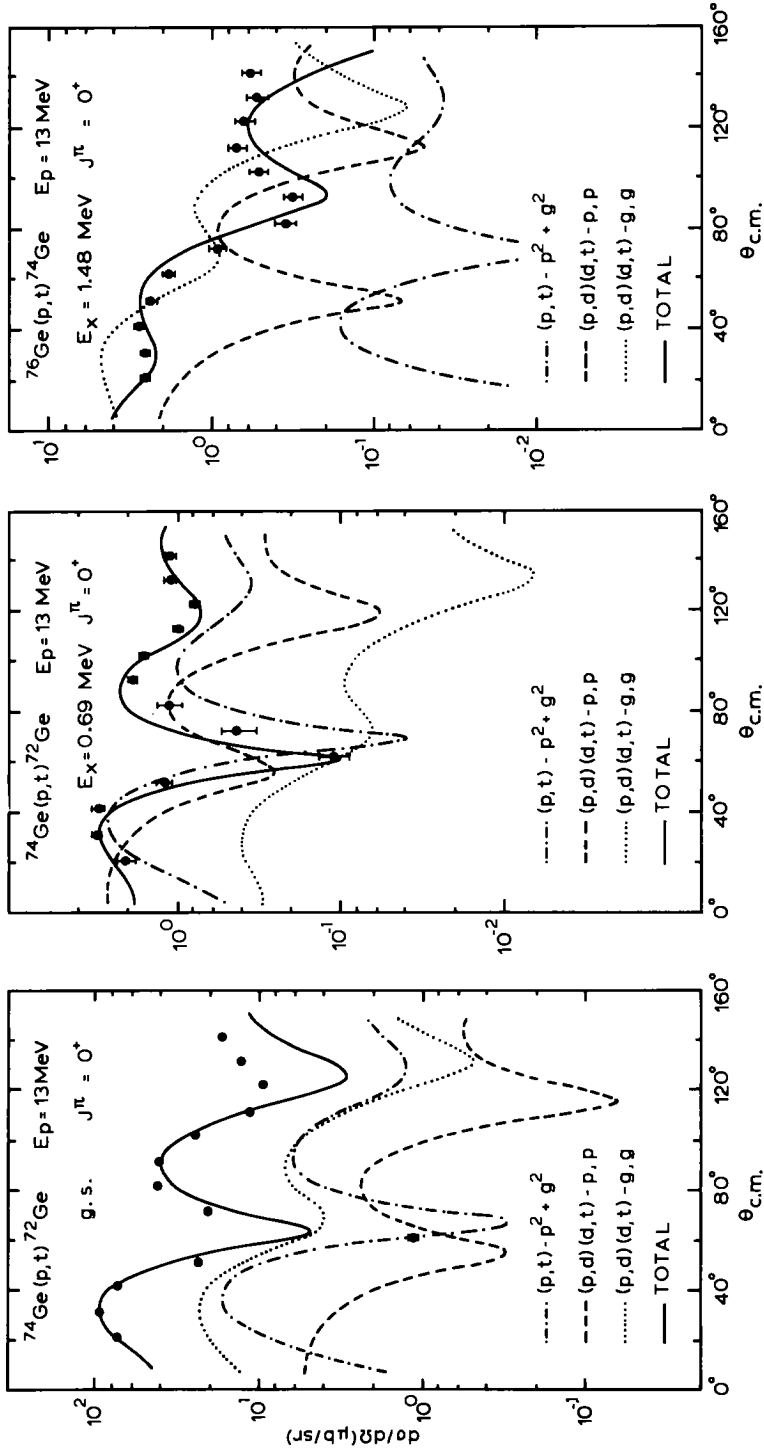
Fig. 5. Individual contributions of one-step and two-step processes to the total cross section for some of the 13 MeV (p, t) angular distributions. The different routes with the structure of the form factors are specified in the figure ($2p_{1/2}$ and $1g_{9/2}$ form factors are abbreviated by p and g, respectively).

be strongly fragmented in reality. In ^{73}Ge a $\frac{9}{2}^+$ level has been found at 0.66 MeV [ref. [29]] and in ^{75}Ge a level at 1.53 MeV [ref. [30]] has been assigned $J^\pi = \frac{7}{2}^+$ or $\frac{9}{2}^+$. The excitation energies of these levels are quite close to the values expected for the $\frac{9}{2}_2^+$ states from the shell-model calculation. Inclusion of the sequential transfer via these states does not strongly affect the angular distribution for the ^{74}Ge(0_2^+) state, while it gives a reasonable improvement for the ^{72}Ge(0_2^+) state. The enhancement factor for this state is reduced to about 1 and the ratio of the cross sections for the second and first maxima is reduced to below the value found experimentally.

5.2. CALCULATIONS IN AN EXTENDED SHELL-MODEL SPACE

To estimate the contribution of other two-neutron configurations to the (p, t) cross section, more extensive shell-model calculations are required. Moreover, such calculations provide an estimate of the reliability of the simple model. Therefore, calculations similar to those of De Vries [27] have been performed. The configuration spaces used in this work are close to the limitations of the present techniques. Two types of calculation were performed. In the first type [named MAXT, following ref. [27]] the $2p_{3/2}$ orbit is assumed to be closed and the neutrons are allowed to occupy the $1f_{5/2}$, $2p_{1/2}$ and $1g_{9/2}$ orbits. No restriction on the configuration spaces were necessary for this model. In the second model (called SSR4) in addition the $2p_{3/2}$ orbit is open for both neutrons and protons. In this model the configuration space had to be truncated in the number of particle distributions [27]. If necessary a second truncation, limiting the sum of the seniorities of the single-shell states to $\nu \leq 7$ (De Vries used $\nu \leq 4$) was used to keep the dimension of the configuration spaces below 1000. The overall agreement of both calculations with experiment is not very good, but the gross properties of the level schemes are reproduced. In particular, the trend of the energies of the first excited 0^+ states is reproduced qualitatively. In ^{72}Ge the 0_2^+ state is indeed the lowest excited state, but it is still calculated about 0.5 MeV too high.

From a comparison of the wave functions of the levels of interest for the different models one learns that the configurations of which the simple model was composed [eqs. (2) and (3)] are also dominant in the wave functions of the MAXT model. Configurations with one or two neutrons excited from the $1f_{5/2}$ orbit contribute 15 to 30%. In the SSR4 model the configurations of the simple model also account for 70 to 85% of the wave functions, but the remaining strength is distributed over many configurations among which configurations with protons promoted from the $2p_{3/2}$ to the $1f_{5/2}$ orbit. For the ^{74}Ge(0_2^+) state only 50% of the SSR4 wave function is represented by configurations of the simple model.

With both sets of wave functions coupled-channels calculations were performed, including, apart from the routes mentioned in subsect. 5.1, also the direct transfer of a $1f_{5/2}^2$ neutron pair and the sequential transfer via the first-excited $\frac{5}{2}^-$ state in the odd isotope. The results did not differ drastically from the calculations with

the simple model, as was already expected from the comparison of the wave functions. The contributions from pickup of the two neutrons from the $1f_{5/2}$ orbit are not very important, due to the small intrinsic strength of these transfer routes. Pickup from the $2p_{3/2}$ orbit which can occur within the SSR4 model turned out to be negligible. Enhancement factors for the calculations with the MAXT and SSR4 models are given in table 1. They agree within a factor of 2 mutually and with the results of the simple model.

6. Description of other reaction data

6.1. ONE-NEUTRON TRANSFER REACTIONS

The most direct information about the wave functions of nuclear states is obtained from single-nucleon pickup or stripping reactions. Therefore, in table 4 a comparison of measured and calculated spectroscopic factors is given for transitions which can be described with the (modified set of) simple shell-model wave functions. The overall agreement is quite reasonable if one takes into account the experimental uncertainties which are reflected in the variations in the results found by different authors. The worst agreement of course occurs for the data involving states of ^{70}Ge or ^{71}Ge, since these nuclei obviously have a too simple structure in our model. The

TABLE 4

Comparison of spectroscopic factors (S) for single-neutron transfer reactions with simple-model calculations

Transition	S_{exp}	S_{calc} [a]
^{70}Ge(d, p)^{71}Ge($\frac{1}{2}^-_1$)	0.29 [b], 0.27 [c], 0.62 [d]	1.0
^{70}Ge(d, p)^{71}Ge($\frac{9}{2}^+_1$)	0.87 [b], 0.73 [c]	1.0
^{72}Ge(p, d)^{71}Ge($\frac{1}{2}^-_1$)	1.04 [e]	1.0
^{72}Ge(p, d)^{71}Ge($\frac{9}{2}^+_1$)	1.93 [e]	1.0
^{72}Ge(d, p)^{73}Ge($\frac{1}{2}^-_1$)	0.16 [f], 0.36 [b], 0.26 [g], 0.39 [h]	0.50
^{72}Ge(d, p)^{73}Ge($\frac{9}{2}^+_1$)	0.52 [c], 0.44 [f], 0.61 [b], 0.50 [g], 0.73 [h]	0.90
^{73}Ge(p, d)^{72}Ge(0^+_2)	<0.003 [e]	0.03
^{74}Ge(p, d)^{73}Ge($\frac{1}{2}^-_1$)	0.56 [e]	0.50
^{74}Ge(p, d)^{73}Ge($\frac{9}{2}^+_1$)	3.35 [e]	2.6
^{74}Ge(d, p)^{75}Ge($\frac{1}{2}^-_1$)	0.42 [b], 0.31 [g], 0.36 [h]	0.25
^{74}Ge(d, p)^{75}Ge($\frac{9}{2}^+_1$)	0.46 [b], 0.43 [g], 0.48 [h]	0.23
^{76}Ge(p, d)^{75}Ge($\frac{1}{2}^-_1$)	0.61 [e]	1.6
^{76}Ge(p, d)^{75}Ge($\frac{9}{2}^+_1$)	4.2 [e]	4.4

[a] The calculated values were obtained from the modified set of wave functions, listed in table 3.
[b] Ref. [3]. [c] Ref. [34]. [d] Ref. [35]. [e] Ref. [2]. [f] Ref. [36]. [g] Ref. [37]. [h] Ref. [38].

^{73}Ge(p, d)^{72}Ge reaction to the 0_2^+ state is worth special attention. The negligible spectroscopic factor found experimentally for this transition is well reproduced by the calculation.

6.2. HIGHER-ENERGY (p, t) AND (t, p) REACTIONS

The availability of angular distributions of the (p, t) and (t, p) reactions on the even Ge isotopes at several incident energies allows a more profound study of the $0^+ \rightarrow 0^+$ transitions in these two-nucleon transfer reactions. The same type of CCBA calculation as was carried out for the 13 MeV data was also performed for the (p, t) reactions at $E_p = 20$ [ref. [5])], 26 [ref. [6])] and 35.4 MeV [ref. [7])] and for the (t, p) reaction at 17 MeV [ref. [19])]. Optical model parameters were again taken from systematic analyses, references for which are listed in table 5. A comparison of the

TABLE 5

References for the optical model parameters [a]) used in the CCBA calculations for the (p, t) and (t, p) reactions on the even Ge isotopes

Reaction	E_{inc} (MeV)	Ref. [b])	p+Ge	d+Ge	t+Ge
(p, t)	20	[5])	[39])	[32])	[33])
(p, t)	26	[6])	[39])	[40])	[33])
(p, t)	35.4	[7])	[39])	[41])	[33])
(t, p)	17	[9])	[39])	[40])	[33])

[a]) All parameter sets were taken from systematic surveys most of which can also be found in ref. [23]).
[b]) References for the experimental data.

calculated and measured angular distributions for the transitions to ^{72}Ge(g.s.), ^{72}Ge(0_2^+) and ^{74}Ge(0_2^+) are given in fig. 6, while a complete list of calculated enhancement factors is given in table 6.

From fig. 6 one sees that the shape of the ^{72}Ge(g.s.) transition (which is also typical for the other ground-state transitions) is well reproduced for all reactions. Some small deviations do occur. Especially for the 26 MeV (p, t) reaction there is a marked difference in the angular region from 15° to 30° which is very sensitive to both the optical potentials and the structure of the form factors. The enhancement factors which for almost all g.s. $\rightarrow$ g.s. transitions are between 1 and 2 are also about 30% higher at 26 MeV. We did not try to improve on these discrepancies by modifying the optical potentials.

The description of the (p, t) transition to the ^{72}Ge(0_2^+) state is slightly worse at $E_p = 20$ and 26 MeV. At 26 MeV the deviation occurs again in the region from 15° to 30°. Both the shape and the enhancement factors for these transitions can be improved by including the sequential transfer route via a second $\frac{9}{2}^+$ state in

TABLE 6

Enhancement factors ($\varepsilon = \sigma_{exp}/\sigma_{calc}$) obtained from CCBA and single-step DWBA calculations for (p, t) and (t, p) reactions on the even Ge isotopes

Reaction / Final state	(p, t) 13 MeV	(p, t)[5] 20 MeV	(p, t)[6] 26 MeV	(p, t)[7] 35.4 MeV	(t, p)[9] 17 MeV
^{70}Ge (g.s.)	0.9 (4.7)	1.7 (4.1)	2.4 (7)	1.8 (2.7)	
^{72}Ge (g.s.)	1.5 (8)	1.9 (11)	1.9 (6)	1.4 (2.7)	1.3 (2.9)
^{72}Ge (0_2^+)	3.6 (4.2)	4.1 (7)	4.5 (5)	1.7 (2.2)	0.06 (0.16)
^{74}Ge (g.s.)	1.6 (4.8)	1.8 (4.1)	2.7 (4.4)	2.1 (2.3)	1.3 (3.8)
^{74}Ge (0_2^+)	1.9 (30)	0.6 (11)	0.43 (4.8)	0.32 (2.8)	1.0 (1.6)
^{76}Ge (g.s.)					1.9 (3.0)

The values between parentheses are enhancement factors for calculations with direct two-nucleon transfer only.

^{73}Ge, as was also the case for the 13 MeV angular distribution. The idea that the origin of the discrepancies found for the ^{72}Ge(0_2^+) state mainly lies in the neglect of other sequential transfer routes is further supported by the fact that the transition to this state is much better described at 35.4 MeV, where the two-step processes are considerably less important, as is evident from a comparison of enhancement factors for the complete CCBA calculations and those for the direct step only (included also in table 6).

The shape of the (p, t) angular distributions for the ^{74}Ge(0_2^+) state is surprisingly well described at all incident energies, if one takes into account the strongly anomalous character of these transitions. Remarkable in this case is that the CCBA enhancement factors become smaller with increasing proton energy. A possible explanation for this phenomenon is that two-step processes via higher excited states in ^{75}Ge contribute (destructively) to this weak transition, which are suppressed at 13 MeV because of the low energy of the deuterons involved in these routes (the Q-value for the ^{76}Ge(p, d)^{75}Ge reaction is −7.2 MeV). On the other hand the constant and rather small values of the enhancement factors for the direct process only for all transitions at 35.4 MeV, where two-step processes are less important, give confidence in the wave functions for the 0^+ states.

The (t, p) transitions to the two 0_2^+ states require some special attention. In (t, p) the transition to ^{74}Ge(0_2^+) is relatively strong and the angular distribution has a normal shape. Both the shape and the absolute cross section ($\varepsilon = 1$) are reasonably well described in the calculation. For the very weak transition to ^{72}Ge(0_2^+) the anomalous character of the angular distribution is reproduced (at least the phase of the oscillation is correct) but the absolute cross section is calculated much too large. The latter deficiency might be attributed to an oversimplification of the ^{70}Ge and ^{71}Ge wave functions in our model.
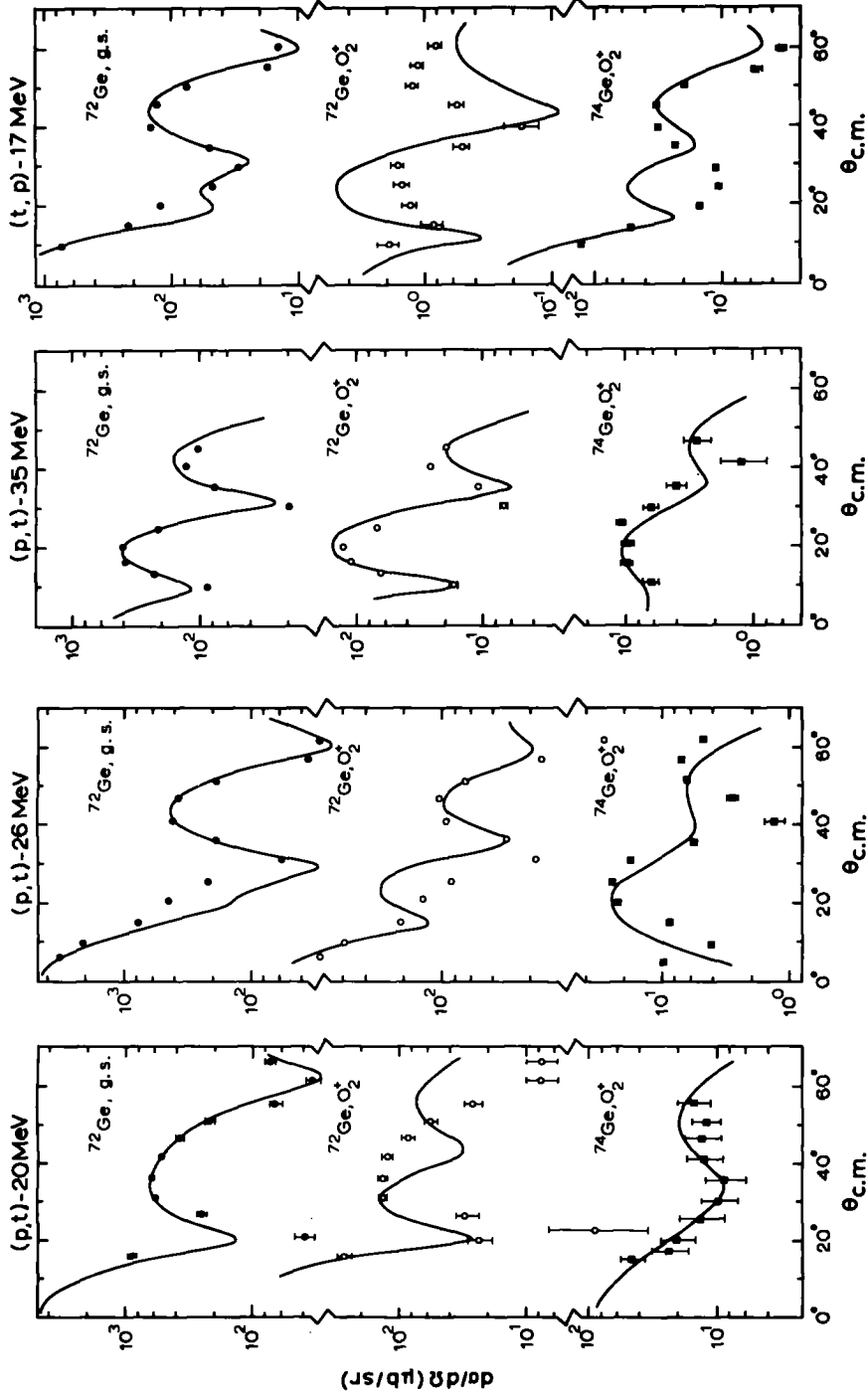
Fig. 6. CCBA calculations with simple shell-model wave functions for the Ge(p, t)Ge reactions at 20 MeV [ref. [5]], 26 MeV [ref. [6]], 35.4 MeV [ref. [7]] and the (t, p) reaction at 17 MeV [ref. [9]]. Scaling factors (ε) for these angular distributions are given in table 6.

6.3. OTHER REACTION DATA CONCERNING THE 0^+ STATES

Recently the first-excited 0^+ states in the Ge isotopes have also been studied by means of the (d, ^{6}Li) [11] and (^{6}Li, d) [12] reactions. The ratios of the strength of the transitions to the 0_2^+ state and the ground state observed in these reactions are listed in table 7. For the calculation of these ratios it was assumed that the Se and Zn ground states can be described by coupling two protons (or proton holes) to the ground states of the corresponding Ge isotone. In that case the α-transfer transition amplitude may be factorized into a two-proton and a two-neutron amplitude [42]. Since the proton structures of the 0_2^+ and 0_1^+ states of the Ge isotopes are

TABLE 7

Relative strengths of transitions to the first-excited 0^+ state and the ground state of Ge isotopes, observed in α-transfer reactions
$R = S(0_2^+)/S(\text{g.s.})$

Reaction	Ref.	R_{exp}	R_{calc} [a]
^{68}Zn(^{6}Li, d)^{72}Ge	[12]	0.09	0.09
^{76}Se(d, ^{6}Li)^{72}Ge	[11]	0.32	0.36
^{70}Zn(^{6}Li, d)^{74}Ge	[12]	0.71	0.54
^{78}Se(d, ^{6}Li)^{74}Ge	[11]	<0.03	0.005

[a] The calculations were performed with the modified set of wave functions from table 3. Wave functions of the Se and Zn isotopes are discussed in the text.

identical in our approach, the strength ratios R are determined by the two-neutron transfer strength according to

$$R = \left[\frac{S^{1/2}(2p_{1/2}^2) + \rho S^{1/2}(1g_{9/2}^2)|0_2^+}{S^{1/2}(2p_{1/2}^2) + \rho S^{1/2}(1g_{9/2}^2)|\text{g.s.}} \right]^2 . \tag{4}$$

The $S^{1/2}$ are two-neutron spectroscopic amplitudes and ρ represents the ratio of the intrinsic DWBA transition amplitudes for transfer to the $1g_{9/2}$ and $2p_{1/2}$ orbits; one finds $\rho = 0.53$ for the (p, t) reaction. The ratios calculated in this way are in very good agreement with the experimental values (see table 7) for both the pickup and the stripping reactions to the ^{72}Ge(0_2^+) and ^{74}Ge(0_2^+) states. Because in α-particle transfer contributions from sequential processes are less likely, this agreement supports our idea that the discrepancies encountered in the analysis of some of the (p, t) and (t, p) transitions at higher incident energies are mainly due to the neglect of some sequential transfer routes.

Data [1,4,43-45] which involve the transfer of an unpaired proton are not as easily explained. Of these especially the ^{71}Ga(^{3}He, d)^{72}Ge reaction [45] is important. The large ratio $\sigma(0_2^+)/\sigma(\text{g.s.}) = 0.6$ observed experimentally in this reaction, which was

one of the main motives for the introduction of orthogonal proton wave functions [1]), cannot be reproduced in our approach, if one considers the ^{71}Ga ground state merely as a proton hole coupled to the ^{72}Ge ground state.

7. Conclusions

The (p, t) reaction leading to 0^+ states in ^{70,72,74}Ge at a low incident energy of 13 MeV has proven to be useful to disentangle the effects of the reaction mechanism and of the structure of the 0^+ states. The sub-Coulomb triton energy enhances the sensitivity of the shape of the angular distributions to the structure of the two-nucleon transfer form factors. At the same time two-step processes appeared to be relatively strong at this energy. On the other hand the number of possible sequential transfer routes is limited by the relatively small range of excitation energies in the intermediate isotope through which these processes can proceed.

Both the shape and the absolute magnitude of the measured $0^+ \to 0^+$ angular distributions could be satisfactorily explained within a coupled-channels approach using simple shell-model wave functions consisting of neutron configurations only. These wave functions comprise the dominant components of the wave functions obtained in more elaborate shell-model calculations and they are in fair agreement with spectroscopic factors for single-neutron transfer. The sequential transfer routes proved to be crucial to explain, especially, the deviations from a "normal" $L = 0$ shape which were observed in the angular distributions for the transitions to the first-excited 0^+ states.

The (p, t) angular distributions at higher incident energies and those for the corresponding (t, p) transitions were also well described in the CCBA approach. Some deviations are probably due to sequential transfer routes via higher excited states in the intermediate isotope which were not taken into account explicitly. For α-transfer reactions to the same states, where multi-step processes are less likely, the ratios of 0_2^+ and 0_1^+ cross sections were reproduced very well.

The results presented in this paper favour a straightforward explanation of the anomalies encountered in connection with the low-lying 0^+ states in the Ge isotopes, which does not support the qualitative interpretation of these anomalies in terms of a coexistence of different nuclear shapes [1,8,9,15]), which has been largely based on the (p, t) and (t, p) data. In another approach [1,12]), where the wave functions of the 0_2^+ and 0_1^+ states are considered to be orthogonal in the proton configurations only, the relative cross sections of the neutron transfer reactions can be explained (in that model some of the experimental data are used to fix the parameters of the wave functions). In addition that model can explain some salient results of proton transfer reactions. On the other hand the anomalous shape of some of the (p, t) and (t, p) angular distributions have not been described within this approach. These shapes appeared to depend crucially on the relative amplitudes of the neutron configurations in the wave functions. Also the 0^+ wave functions obtained from

the SSR4 shell-model calculation (see sect. 5), which does allow for proton excitations from the $1f_{5/2}$ orbit, do not contain such proton configurations with an appreciable amplitude.

In conclusion we think that a complete description of the structure of the low-lying 0^+ states should at least include neutron configurations in a combination which is considerably different for the ground state and the excited state.

References

1) M. Vergnes, Proc. 6th Eur. Phys. Soc. Nucl. Div. Conf. on structure of medium-heavy nuclei, Rhodos (1979), Inst. Phys. Conf. Ser. No. 49, Bristol and London (1980) p. 25
2) R. Fournier, J. Kroon, T.H. Hsu, B. Hird and G.C. Ball, Nucl. Phys. A202 (1973) 1
3) W.A. Yoh, S.E. Darden and S. Sen, Nucl. Phys. A263 (1976) 419
4) G. Rotbard, G. La Rana, M. Vergnes, G. Berrier, J. Kalifa, F. Guilbault and R. Tamisier, Phys. Rev. C18 (1978) 86
5) G.C. Ball, R. Fournier, J. Kroon, T.H. Hsu and B. Hird, Nucl. Phys. A231 (1974) 334
6) F. Guilbault, D. Ardouin, J. Uzureau, P. Avignon, R. Tamisier, G. Rotbard, M. Vergnes, Y. Deschamps, G. Berrier and R. Seltz, Phys. Rev. C16 (1977) 1840
7) A.C. Rester, J.C. Ball and R.L. Auble, Nucl. Phys. A346 (1980) 371
8) D. Ardouin, C. Lebrun, F. Guilbault, B. Remaud, E.R. Flynn, D.L. Hanson, S.D. Orbesen, M.N. Vergnes, G. Rotbard and K. Kumar, Phys. Rev. C18 (1978) 1201
9) C. Lebrun, F. Guilbault, D. Ardouin, E.R. Flynn, D.L. Hanson, S.D. Orbesen, R. Rotbard and M.N. Vergnes, Phys. Rev. C19 (1979) 1224
10) S. Mordechai, H.T. Fortune, R. Middleton and G. Stevens, Phys. Rev. C18 (1978) 2498 and C19 (1979) 1733
11) A.M. van den Berg, R.V.F. Janssens, G.T. Emery, A. Saha and R.H. Siemssen, Nucl. Phys. A379 (1982) 239
12) D. Ardouin, D.L. Hanson and Nelson Stein, Phys. Rev. C22 (1980) 2253
13) S. Hinds, J.H. Bjerregaard, O. Hansen and O. Nathan, Phys. Lett. 14 (1965) 48; J.H. Bjerregaard, O. Hansen, O. Nathan and S. Hinds, Nucl. Phys. 86 (1966) 145
14) J.R. Maxwell, G.M. Reynolds and N.M. Hintz, Phys. Rev. 151 (1966) 1000; D. Debenham and N.M. Hintz, Phys. Rev. Lett. 25 (1970) 44
15) M.N. Vergnes, G. Rotbard, F. Guilbault, D. Ardouin, C. Lebrun, E.R. Flynn, D.L. Hanson and S.D. Orbesen, Phys. Lett. 72B (1978) 447
16) Y. Iwasaki, T. Murata, T. Tamura and Y. Nogami, Phys. Rev. C13 (1976) 556
17) A. Becker, E.A. Bakkum and R. Kamermans, Phys. Lett. 110B (1982) 199
18) H.W. Fulbright and J.R. Erskine, Nucl. Instr. 162 (1979) 355
19) T.H. Curtis, H.F. Lutz and W. Bartolini, Phys. Rev. C1 (1970) 1418
20) C.M. Perey, F.G. Perey, J.K. Dickens and R.J. Silva, Phys. Rev. 175 (1968) 1460
21) R. Stokstad, Yale University Report No. 52 (1972)
22) P.D. Kunz, University of Colorado, unpublished
23) C.M. Perey and F.G. Perey, Atomic Data and Nucl. Data Tables 17 (1976) 2

24) B.F. Bayman and A. Kallio, Phys. Rev. **156** (1967) 1121
25) L.C. Biedenharn and M.E. Rose, Rev. Mod. Phys. **25** (1953) 729
26) E.U. Condon and G.H. Shortley, The theory of atomic spectra (Cambridge University Press, 1953)
27) H.F. de Vries, Ph.D. Thesis, University of Utrecht (1976), unpublished
28) P.J. Brussaard and P.W.M. Glaudemans, Shell-model applications in nuclear spectroscopy (North-Holland, Amsterdam, 1977)
29) L.P. Ekström and F. Kearns, Nucl. Data Sheets **29** (1980) 1
30) L.P. Ekström, Nucl. Data Sheets **32** (1981) 211
31) F.G. Perey, Phys. Rev. **131** (1963) 745
32) J.M. Lohr and W. Haeberli, Nucl. Phys. **A232** (1974) 381
33) F.D. Becchetti, Jr. and G.W. Greenlees, in Polarization phenomena in nuclear reactions, ed. H.H. Barschall and W. Haeberli (University of Wisconsin Press, Madison, Wisconsin, 1971) p. 682
34) L.H. Goldman, Phys. Rev. **165** (1968) 1203
35) V.F. Litvin, Yu.A.Nemilov, K.A. Gridnev, K.J. Zherebtsova, L.V. Krasnov, V.A. Komarov, Yu.A. Lakomkin, T.V. Orlova, V.P. Bochin, V.S. Romanov and S.A. Repin, Sov. J. Nucl. Phys. **6** (1968) 501
36) G. Heymann, P. van der Merwe, J.J. van Heerden and I.C. Dormehl, Z. Phys. **218** (1969) 137
37) N. Kato, Nucl. Phys. **A203** (1973) 97
38) A. Hasselgren, Nucl. Phys. **A198** (1972) 353
39) F.D. Becchetti, Jr. and G.W. Greenlees, Phys. Rev. **182** (1969) 1190
40) J.D. Childs, W.W. Daehnick and M.J. Spisak, Phys. Rev. **C10** (1974) 217
41) C.M. Perey and F.G. Perey, Phys. Rev. **152** (1966) 923
42) D. Kurath and J.S. Towner, Nucl. Phys. **A222** (1974) 1
43) M. Vergnes, G. Rotbard, J. Vernotte, G. Berrier and C. Lebrun, Proc. 6th Eur. Phys. Soc. Nucl. Div. Conf. on structure of medium-heavy nuclei, Rhodos (1979), Inst. Phys. Conf. Ser. No. 49, Bristol and London (1980) p. 228
44) D. Ardouin, R. Tamisier, G. Berrier, J. Kalifa, G. Rotbard and M. Vergnes, Phys. Rev. **C11** (1975) 1649
45) D. Ardouin, R. Tamisier, M. Vergnes, G. Rotbard, J. Kalifa, G. Berrier and B. Grammaticos, Phys. Rev. **C12** (1975) 1745